Materials and Design 186 (2020) 108206

Contents lists available at ScienceDirect

Materials and Design

journal homepage: www.elsevier.com/locate/matdes

Achieving coalesced breathability, mechanical and shape memory properties of collagen fibrous matrix through complexing with chromium (III)

Yanting Han [a], Yuanzhang Jiang [a], Jinlian Hu [a,*], Xiaoyu Chen [b]

[a] Institute of Textiles and Clothing, The Hong Kong Polytechnic University, Hong Kong, China
[b] Department of Biomedical Engineering, The Chinese University of Hong Kong, Hong Kong, China

HIGHLIGHTS

- Organic-metal biosystem developed retains inherent conformation of collagen and its fiber morphology in the skin.
- Cr-CFM exhibits enhanced waterproofness, breathability and mechanical adaptability.
- Cr-CFM achieves a water-responsive shape memory ability with shape fixation and recovery reaching over 80%.
- Hydrogen bonds facilitate shape deformation while chromium (III) complexing linkages promote shape recovery.

GRAPHICAL ABSTRACT

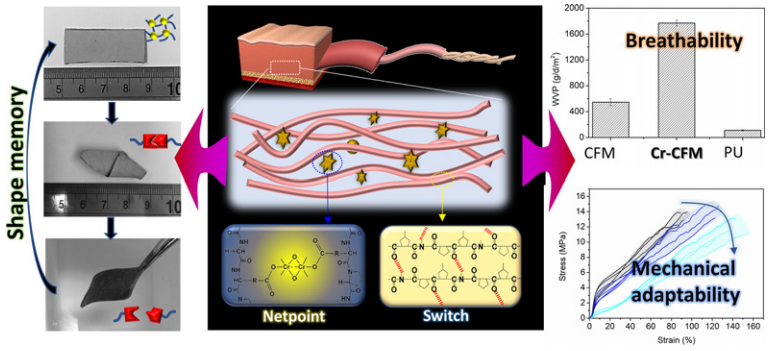

ARTICLE INFO

Article history:
Received 28 May 2019
Received in revised form 9 August 2019
Accepted 10 September 2019
Available online 12 September 2019

Keywords:
Collagen fibrous matrix
Chromium complexing
Shape memory
Coalesced properties

ABSTRACT

Protein materials evolved in nature for millions of years can display critical structural and functional properties which is difficult for synthetic polymers to surpass. Hence, the combination of multiple components or hierarchies from natural source through a facile method may stand out as a forerunner to materials design and application. Inspired from metalloprotein, this study reported an organic-metal biosystem based on chromium (III) complexed collagen fibrous matrix (Cr-CFM). The obtained Cr-CFM retains inherent conformation of collagen and its fiber morphology in the skin. Compared with pristine CFM, Cr-CFM showed enhanced waterproofness and breathability. Due to coexistence of hydrogen bonds and newly introduced chromium (III) complexing linkages, Cr-CFM exhibited water-adaptive mechanical property. In this organic-metal biosystem, hydrogen bonds show reversible cleavage-reformation under water interference while chromium (III) complexing linkages remains stable. Such combination of "switch" and "netpoint" facilitated water responsive shape memory ability of Cr-CFM with shape fixation and recovery reaching over 80%. The reveal of relationship between structure and coalesced properties of Cr-CFM herein is believed to promote progress of smart protein materials and give inspirations to synthetic polymers.

* Corresponding author.
E-mail address: jin-lian.hu@polyu.edu.hk (J. Hu).

https://doi.org/10.1016/j.matdes.2019.108206

1. Introduction

As the fundamental building blocks of vast array of biological materials, protein is responsible for many critical functions of life. Their properties mainly depend on its amino acid sequence and hierarchical assembles [1]. Generally, amino acids have different physicochemical properties and side chains in various spatial arrangement, which can promote self-assembly and formation of structural hierarchy of polypeptide with different sequence [2]. The resulted characteristic conformation includes α helix, β sheet, triple helix and random coil [3]. These structures can exist in biological tissues either alone or simultaneously to perform specific functions. Bones, skin and natural silk are examples of materials that have integrated elasticity, strength, and robustness unmatched by many synthetic materials. Fortunately, some protein materials are available in large quantities in nature, and thus can be directly utilized by human. Among them, collagen is one of the most abundant protein found in animal body.

Collagen has a unique right-handed triple helical structure composed of three intertwined left-handed α helices. Such 3-dimentional conformation can dynamically adapt to load application by self-organization and self-arrangement. Since collagen has excellent biological (e.g. biocompatibility, low antigenicity and biodegradability) and physical properties (e.g. mechanical strength, structural stability) [4,5], researches have tried to extract collagen from tissues and prepare collagen-based materials for various applications [6]. Fibers and films are common forms of these reconstructed collagen-based materials [7,8]. It is believed that the closer to natural state, the better the performance of biomaterials [9], however, processes of extraction or spinning would destroy structure of collagen to a certain extent due to solvent-induced hydrolysis effect, not to mention the formation of a tissues-analogous hierarchical structure. An alternative method for preserving original collagen assembles is to remove non-collagen component from target tissue. One of the successful examples is preparation of collagen-based materials from animal skin [10]. Specifically, as essential structural component in skin, collagen naturally grows into a unique fibrous structure which aims to provide skin with toughness, ductility and permeability, as well as maintain skin appearance. Many artificial materials are designed to mimic such fibrous matrix [11]; however, their performance is not comparable to the natural one due to their lack of integrated features from composition to structure. Hence, products prepared by methods including decellularization and electrospinning [12,13], which retain fibrous structure of skin, such as decellularized dermal scaffolds [14], wound dressings [15], grafting [16] have an unsurpassed and irreplaceable position since they meet the sophisticated requirements in practical applications. Nevertheless, compared to other natural biomass materials (e.g. cellulose [17]) which have been extensively studied for various applications, research on collagen-based materials is largely limited to biomedical field. Hence, this study aims to reveal the new functionals of collagen-based materials from other application perspective, which may bring new insights to this type of natural materials.

More recently, we found that collagen has intrinsic water adaptive ability, namely the self-assembly of collagen fibers through cleavage and reforming of abundant hydrogen bonds (H-bonds) within peptide chains [18,19]. This kind of behavior is similarly to mechanism of some smart materials, such as shape memory materials of which the existence of reversible bonds plays an essential role [20]. Generally, mechanism governing shape memory effect of polymers can be explained by a netpoint-switch model where netpoint determines permanent shape while reversible bonds act as switches to allow temporary shape change [20]. In this case, collagen-based material possesses native "switch" element for realizing shape memory ability, while the challenge lies on introducing suitable cross linkages as "netpoint" into collagen matrix for stabilization of permanent shape. Metalloproteins containing stable protein metal-binding sites [21] give us inspiration that generation of organic-metal complex may provide a feasible approach to endow structural protein materials with more specific functions. Such hybrid system may also lead to complete set of properties and bring new understanding of smart functionality of protein materials. According to Valence bond theory [22], chromium (III) can form inner orbital complex with collagen peptides [23,24]. Other research found that chromium (III) created DNA-protein crosslinks by binding with reactive amino acids [25] while other metals such as Ni (II) cannot participate directly in the DNA-protein crosslinks [26]. Thus, compared with other metals (e.g. aluminum (III), iron (III), zinc (II), etc.), the hybrid of chromium (III)-collagen system can provide a stable platform as the research object. Besides, chromium (III) can be multi-point bonded with carboxyl group on peptide chain [25]. Such structure may lead to novel properties of final product, which remains to be studied.

Herein, we proposed organic-metal biosystem where chromium (III) was chosen to complex with collagen to establish a reliable model for investigation of functionalized collagen fibrous matrix. The obtained Chromium (III) complexed collagen fibrous matrix (Cr-CFM) possesses complete skin fibrous structure and preserves collagen conformation, together with coalesced breathability, mechanical and water-responsive shape memory ability. The in-depth investigation of mechanism behind these functions were also conducted from macro structure to molecule levels. The establishment of such hybrid bio-model may promote utility of collagen fiber as a treasured resource for bio-based materials, benefit tunable protein functionalization, as well as give inspirations to invent or perfect the synthetic polymers.

2. Experiment

2.1. Materials and preparation of Cr-CFM

The pickled calfskin (pH of 2.8–3) with all non-collagen substances removed was obtained from local tannery. Basic chromium sulphate (HG/T2678-2007) was purchased from Zhenhua Chemical, China. Formic acid and sodium carbonate were supplied from J&K chemical Hongkong. Laboratory-made deionized water was used throughout.

Collagen fibrous matrix (CFM) was obtained by washing the pickled calfskin several times to remove acid and salts. To prepare the chromium complexed CFM (Cr-CFM), pickled calfskin was treated with basic chromium sulphate 6–8% (on weight of calfskin) with 150% of water (on weight of calfskin) as the bath medium. Formic acid (85%) diluted and added to the bath to adjust pH to 2.5–3 which is beneficial to the loosening of collagen fibrous network, exposing of reactive groups on collagen, as well as penetration of chromium sulphate to promote the later reaction. In this step, color of cross-section of specimen was examined at certain intervals to ascertain the penetration degree of chromium sulphate. Upon completion of penetration, 10% alkali solution was added to the bath to raise pH to 3.8–4.0 to trigger the complexing reaction [23]. After 5 h of reaction at temperature of 38–40 °C, the specimen was taken out and rinsed with 300% water (on weight of calfskin) for 40 min each time. Herein, after three times rinsing, the water becomes transparent, which indicate complete cleaning of specimen according to visual colorimetry. The obtained CFM and Cr-CFM with a thickness of 1.5–2 mm was vacuum dried before testing. The hierarchical fibrous network and proposed chromium-collagen complexing structure of Cr-CFM is illustrated in Fig. 1a. Generally, CFM has a natural fibrous network formed by interlaced collagen fiber bundle which composed of collagen fibril with a parallel staggered array of collagen molecules. The molecular conformation of collagen triple helix confers strict amino acid sequence of α helix chains.

2.2. Materials characterization

Characteristic molecular structure of CFM and Cr-CFM were examined using Fourier Transform spectroscopy (Perkin Elmer Spectrum 100, USA). The morphology of samples was observed by a scanning electron microscope (TESCAN VEGA3). Elemental analysis of selected area

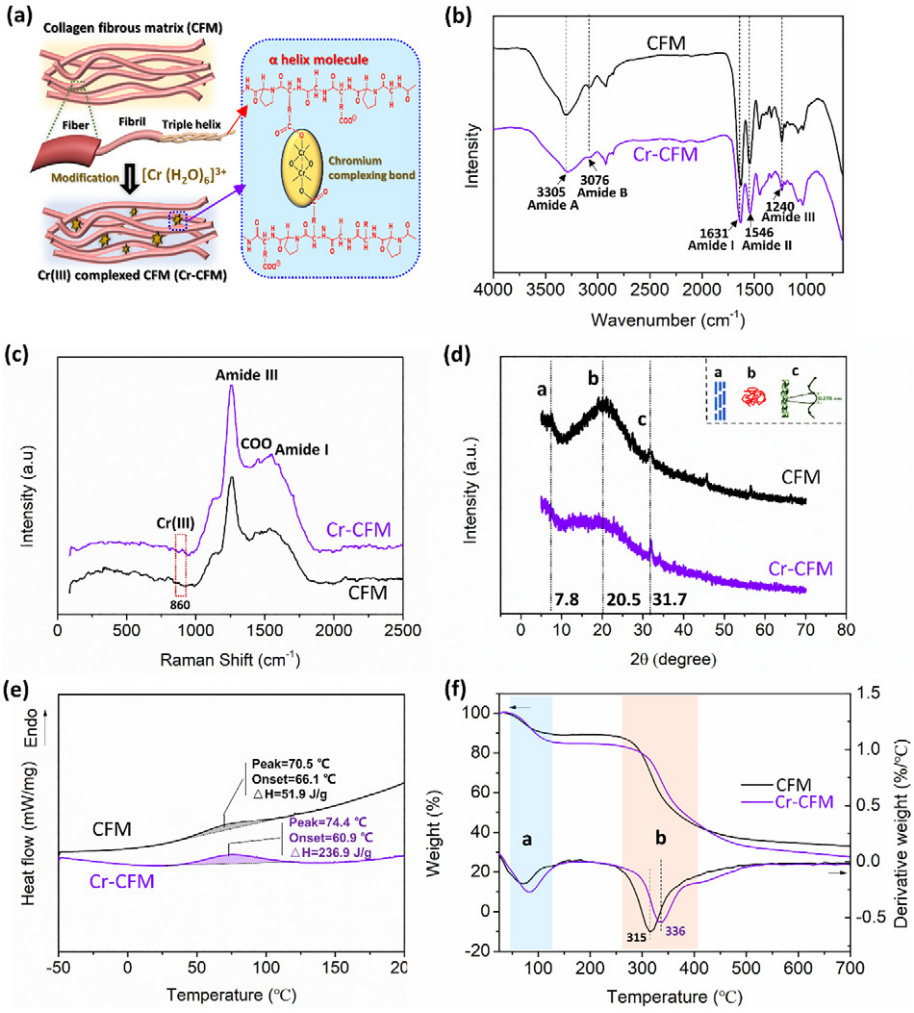

Fig. 1. Structural characterization of CFM and Cr-CFM: (a) scheme of proposed hierarchical network and molecules structure; (b) FTIR spectra; (c) Raman spectra; (d) XRD patterns; (e) DSC characterization; (f) thermal decomposition analysis.

in sample was obtained by using EDS attached to SEM. Simulation of molecular chain was conducted by using ChemDraw 8.0. Porosity analysis based on SEM images of CFM and Cr-CFM was proceeded by ImageJ. The crystal and amorphous structures of samples were investigated by Rigaku Smart Lab XRD system (9 kW) that is equipped with Cu Kαradiation with a wavelength of 1.54 Å. The 2θ range was from 3° to 70°. Thermal stability of samples against time from 25 °C to 700 °C with a heating rate of 10 °C/min was measure using a thermal analyser (METTLER TOLEDO, USA). Water contact angles on CFM and Cr-CFM were tested by the OCAH200 high-speed video contact angle measurer (DataPhysics Instruments GmbH Ger, Filderstadt, Germany). The water vapor permeability (WVP) of samples was measured by ASTM E96 Procedure A-Desiccant method through a Haida International chamber (Model-HD-E702-100-4, Dongguan, China) with controlled function of constant temperature (25 °C) and relative humidity (50%). Briefly, the mouth of a jar containing water was sealed by sample. The initial weight (M_0) of the jar was recorded before placed into chamber. After several hours (t), the jar was taken out and the final weight (M_1) was measured. The mouth of jar as the testing area (S) was calculated. WVP, calculated by equation of $WVP = (M_1\text{-}M_0)/(S \times t) \times 24$, means the weight change of jar through the unit area of sample per day ($g/m^2 \cdot d$). Water swelling ratio (WSR) of samples was determined use equation $WSR = (W\text{-}W_0)/W_0 \times 100\%$ where W is the weight of swollen sample at different times and W_0 attributes to the weight of dried one. Mechanical properties of CFM and Cr-CFM with a length of 10 mm and width of 5 mm were measured by using Instron 5566 at an elongation rate of 50 mm/min. Shape memory ability of samples was qualitative studied. Straight Cr-CFM was wetted and deformed into a helix shape which was fixed after drying. To triggering recovery, sample was immersed into water again. The shape change of sample during testing was recorded by camera. For quantitative characterization of shape memory ability of CFM and Cr-CFM, cyclic tensile testing according to previous research [27] was performed on samples using an Instron 5566. Briefly, the wetted sample was elongated to a certain value of strain (ε_1). The extended sample is dried and fixed at room temperature for 12 h. After removed the load, strain would decrease to a value of ε_2. Then the sample is immersed in water again to allow full recovery. Accordingly, the uncovered strain would decrease to ε_3. The onset of next tensile was from ε_3 to ε_1. The shape fixation ratio (R_f) and shape recovery ratio (R_r) was calculated respectively by equation: $R_f = \varepsilon_2/\varepsilon_1$, $Rr = (\varepsilon_1\text{-}\varepsilon_2(N))/\varepsilon_2(N\text{-}1)$. N represents the Nth cycle of the programming. Shape memory ability of Cr-CFM was also studied by bending cyclic test. The straight sample with original angle (θ_0) of 0° was wetted and bended to the setting angle (θ_s) of 90°. The fixed angle (θ_f) without constrains was measured after drying at 40 °C for 3 h. Then, sample was immersed in water at 25 °C for 40 min for fully triggering of shape recovery to a certain angle (θ_r). R_f and R_r which were calculated by equations of $R_f = \theta_f/\theta_s$ and $R_r = (\theta_r\text{-}\theta_s)/(\theta_0\text{-}\theta_s)$ respectively. The modulus of Cr-CFM under drying and wetting condition with increasing of temperature was tested under the Metter Toledo

DMA operated in 1 Hz with a sample gauge of 10 mm in length and 5 mm in width.

3. Results and discussions

3.1. Structure and morphology analyses

As shown in FTIR spectra (Fig. 1b), typical absorption bands of collagen can be observed on CFM and Cr-CFM. Specifically, peaks at 3305 cm^{-1} and 3087 cm^{-1} are associated with amide A and B bands respectively due to stretching vibrations of N—H. Amide I band associated with stretching variations of C═O is found at 1631 cm^{-1}, while Amide II deriving from rom N—H bending and C—N stretching can be observed at 1546 cm^{-1}. There is a strong peak at 1240 cm^{-1} which is assigned to C—N stretching and N—H bending vibrations from amide III, as well as wagging vibrations of CH_2 groups in glycine backbone and proline side chains [28]. These characteristic bands qualitatively verify collagen molecular structure of both CFM and Cr-CFM. To quantify the degree of triple helix preservation following chromium complexing treatment, FTIR absorption ratio of amide III to 1450 cm^{-1} band (A_{III}/A_{1450}) was determined in both CFM and Cr-CFM. The A_{III}/A_{1450} of CFM is 1.13, consisting with previous research results [29]. As in the case of Cr- CFM, a lowered amide ratio ($A_{III}/A_{1450} = 0.95$) was found. The decrease may be resulted from slightly hydrolysis of collagen in acidic environment. It is recognized that the ratio (A_{III}/A_{1450}) of approximately 1.0 reveals triple-helical structure of collagen since the ratio for denatured collagen (gelatin) is ≈0.6 [30]. Thus, the results indicate that the triple helix conformation of Cr-CFM is not destructed by chromium. In other words, chromium can complex with collagen but without destroying its backbone structure. Fig. 1c shows the Raman spectra of CFM and Cr-CFM. According to literature values [19], peaks ascribed to vibrations of amide I (1640 cm^{-1}) and amide III (1246 cm^{-1}) are identified. Bands corresponding to COO (1421 cm^{-1}) which comes from aspartate and glutamate are also observed. These functional groups represent the donor and acceptor of hydrogen bonds within collagen. Notably, compared to CFM, Cr-CFM exhibits a small new peak at 860 cm^{-1} which arises from the Cr (III) [31,32] attached to the collagen.

Microstructure of CFM and Cr-CFM were examined by X-ray diffraction, as shown in Fig. 1d. There is a small peak (a) at 2θ angles around 7.8° related to intermolecular lateral packing of collagen molecules while the broad peak (b) at $2\theta = 22°$ corresponds to amorphous scatter arises from random coils. Besides, a small peak (c) can be observed at $2\theta = 31°$ which attributes to periodicity of axial rise per residue [33]. These peak positions of CFM and Cr-CFM are consistent, indicating their structural similarity. Nevertheless, Cr-CFM shows a lower intensity of peak (b) than CFM, implying its decreased amount of amorphous region which may result from complexing of chromium that lead to higher crosslinking order of Cr-CFM. As shown in DSC results (Fig. 1e), a broad peak is detectable from temperature around 60 °C. Such change in heat capacity involves in unfolding of individual α helices into random coils of collagen [34]. Specifically, transition peak for CFM is found at 70.5 °C with △H of 51.9 J/g. After chromium complexing, the peak of Cr-CFM shifted to a higher temperature region of 74.5 °C with △H of 236.9 J/g. The shifting in transition temperature and increased enthalpy prove the existence of strong interactions between chromium and collagen which can enhance cohesive energy between peptide molecules and benefit structural stability of collagen matrix [24,35]. Herein, thermal stability study was conducted, and results are shown in Fig. 1f. TGA curves of CFM and Cr-CFM exhibit two stages of thermal degradation process. The first stage starting from ~50 °C is due to release of water molecules working as structural bonds within α helix. It is reported that in addition to self-sufficient hydrogen bonds, the "water bridge bond" also contributes to configuration stability of triple helix [36]. Another main stage starting from ~250 °C corresponds to beginning of collagen decomposition [19]. These two stages can be clearly distinguished from DTGA curves where two corresponding peaks are observed. The value of peak represents maximum decomposition rate. During the first stage, Cr-CFM shows a higher release rate of water molecules than CFM. This may be because that chromium occupied the groups (e.g. COO) which can form hydrogen bonds with water, weakening the interactions between collagen and water molecules. For decomposition of collagen matrix, the rate of Cr-CFM is slower than that of CFM. The horizontal axis of the peak represents temperature corresponding to the maximum decomposition rate. It is found that Cr-CFM (336 °C) has a higher decomposition temperature than CFM (315 °C). Therefore, Cr-CFM exhibited a superior thermo-stability compared with CFM, which can benefit its application in specific fields, particularly under high temperature condition.

SEM images of cross section for CFM (Fig. 2a) and Cr-CFM (Fig. 2b) both show unique fibrous structure with nonwoven-analogous features. It can be seen that collagen fibers are intertwined to form a fibrous network where the fiber bundles are aligned either in the plane or nearly vertical to the plane. Such fiber alignment leads to a 3D structure with voids in CFM (Fig. 2a). After complexing with 3.83% Cr (element weight ratio), the fibrous structure becomes looser while the collagen fiber alignment remains barely change (Fig. 2b). EDS analysis was applied in the selected area of CFM and Cr-CFM to characterize their elemental composition. Strong peaks of C, N and O which are basic elements of collagen protein, were detected in both CFM and Cr-CFM and show similar content proportions. It is noticed that in the spectrum of Cr-CFM, a new peak attributed to element of Cr appeared, confirming presence of chromium. Previous researches have proved that Cr can react with COOH on collagen. The resulted multidentate coordination can be regarded as bridge bond between peptide chains [25,26]. Accordingly, theoretical and simulative molecular structure of Cr-CFM is illustrated in Fig. 2c1 and c2 respectively, which demonstrate rationality of the formation of chromium-collagen complex that can works as "bridge bond" between two polypeptide chains to generate a cross-linked network. From Fig. 2d1, the intertwining of collagen fibers of Cr-CFM can be observed. The highly ordered fibrils are more clearly in the high magnification images of individual fiber bundles (Fig. 2d2 and d3). Particularly, the distinctive D-period structure with alternative dark (about 0.4 D overlap) and light banding (about 0.6 D gap) patterns [37] can be observed from collagen fibril, implying the retaining of bio-inherent hierarchical structure. In other words, polypeptide chains of Cr-CFM can maintain their native helical conformation and packed together in a definite and ordered structure, which is an important trait that distinguishes it from other synthetic materials.

3.2. Breathability

The surface contact angles (CA) of CFM and Cr-CFM were evaluated. Results (Fig. 3a) showed that CA of CFM gradually decreased with time due to its high hydrophilicity and absorption of fibrous matrix. As expected, chromium complexing can significantly improve waterproofness as the CA of Cr-CFM showed minor changes over time. Particularly, CA of Cr-CFM still maintained at ~120°. Previous research provide that chromium complexing would consume hydrophilic group of carboxyl on collagen [25]. And content of carboxyl group can affect the hydrophilicity of the material. Thus, the superior water resistance of Cr-CFM which may result from its compact surface structures and reduced content of hydrophilic groups exposed on surface. Water vapor permeability (WVP) is related to breathable property of materials. Higher WVP allows transmission of water vapor away from body easily, which benefits wearing comfort. Herein, WVP of CFM and Cr-CFM was investigated. As shown in Fig. 3b, WVP of Cr-CFM is four times that of CFM. Meanwhile, compared to commercial polyurethane which are common breathable film products, Cr-CFM shows outstanding WVP performance. The increased WVP of Cr-CFM may resulted from its enhanced porosity. The results suggest that Cr-CFM is able to exclude water at room temperature but allow air and water vapor to

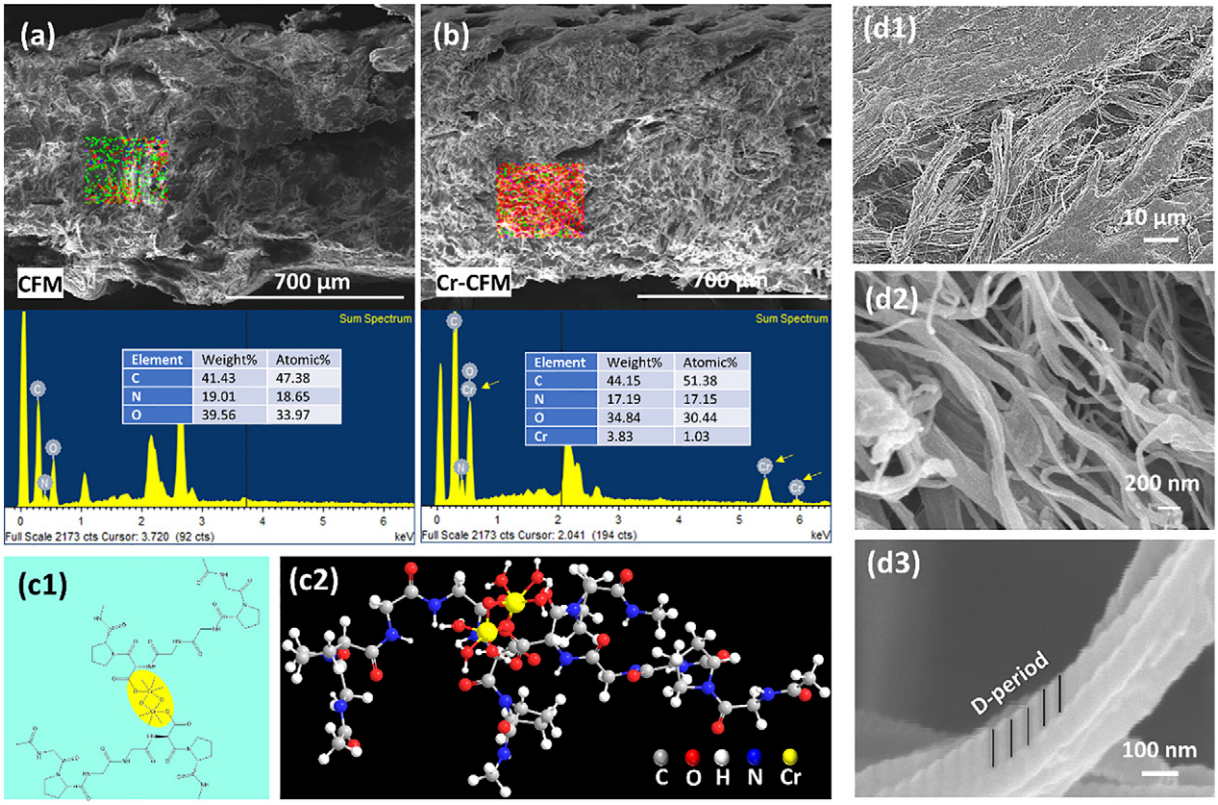

Fig. 2. SEM images and EDS spectra of (a) CFM and (b) Cr-CFM; (c1) proposed molecules structure and (c2) simulation of chromium-collagen complexing chain; SEM images of hierarchal structure of Cr-CFM: (d1) nonwoven analogous network; (d2) assembly collagen fibril; (d3) individual collagen fibral with axial D-periodicity.

pass through the cross section. Such unsurpassed breathability of Cr-CFM may come from its natural fibrous porous structure since capturing, penetration and diffusion of water vapor are important aspects to enhance water vapor permeability [38].

Fig. 3c shows that water swelling ratio (WSR) of CFM increased with immersing time and reached an equilibrium WSR of 400%. In comparison, WSR of Cr-CFM increased fast at beginning and reached the final equilibrium WSR of 70% which is much smaller that of CFM, indicating the decreased water loading property of Cr-CFM. This may due to that chromium-collagen bonding improved the crosslinking of collagen network, restricting the stretching of collagen chains and limits further penetrating of waters and volume expansion. In order to determine the nature of water diffusion process which contributes to water-responsive property, kinetic analysis of CFM and Cr-CFM with a second-order equation [39] was conducted as shown below:

$$dW/dt = k(W_e - W_t)^2 \quad (1)$$

where W, W_e and k denote the degree of swelling at any time (t), degree of swelling at equilibrium, and swelling rate constant, respectively. Integration of Eq. (1) gives the following equation:

$$t/W = A + Bt \quad (2)$$

Herein, $A = 1/k^2$, $B = 1/W_e$. And A and B are the intercept and slope of (t/W)~t relationship curve respectively. Graphs were plotted against (t/W) and t (Fig. 3d) to examine the above kinetic model. The value of k was calculated based on the fitting curve. It is showed that theoretical fitting curves are consistent with experimental results, which confirms that their swelling behavior is in accordance with swelling secondary kinetic equation. The calculated k for CFM and Cr-CFM is 3.07 and 5.477 respectively. That means Cr-CFM has higher swelling rate and thus to reach equilibrium state quickly. This relative fast water take-up capacity benefits the quick responsiveness to water, such as water vapor permeability. In addition, the porous structure is proved to facilitate water penetration and diffusion. This is evidence as shown in Fig. 3e where the porosity of CFM and Cr-CFM was calculated based on the SEM results. It shows that Cr-CFM has a higher porosity than CFM. Hence, external water molecules can penetrate the matrix quickly through three-dimensional (3D) microvoid and get accumulated to reach an equilibrium. This process can generate osmotic pressure and swelling force which is reported to conducive to shape recovery of water responsive materials [40]. Accordingly, the structural model of Cr-CFM regarding to its waterproofness and breathability is shown in Fig. 3f.

3.3. Mechanical properties

Stress-strain curves of CFM and Cr-CFM are shown in Fig. 4a. It is notable that CFM behaves stiffly with high Yong's modulus, which may due to its tight and dense fiber structure in dry state, as well as interactions between fibers including hydrogen bonding, cross-linking, electrovalent bonding, van der Waals force, shear force, etc. [41]. In comparison, Cr-CFM exhibit integrated strength and ductility. The mechanical behaviors of Cr-CFM may be the result of its fibrous structure and newly introduced cross-linking netpoints. Elastic modulus as a function of stain applied to CFM and Cr-CFM are plotted in Fig. 4b. For CFM, three regions with distinct characteristic moduli are identified (referred as Mod 1, Mod 2 and Mod 3), consistent with previous findings [42,43]. The first 5% of deformation led to highest modulus value (Mod 1), after which modulus reduced significantly to lowest value at 13% extension (Mod 2). As strain continuous increase, young's modulus gradually raised to another peak at strain of 38% (Mod 3) before final decrease stage. It is recognized that tensile behavior of materials with fibrous structure involves several stages (illustrated in insert figure): straightening of wavy fibers, stretching and slippage of crosslinked fibers, and defibrillation and breaking of fibrils [42,44]. Fig. S1 shows

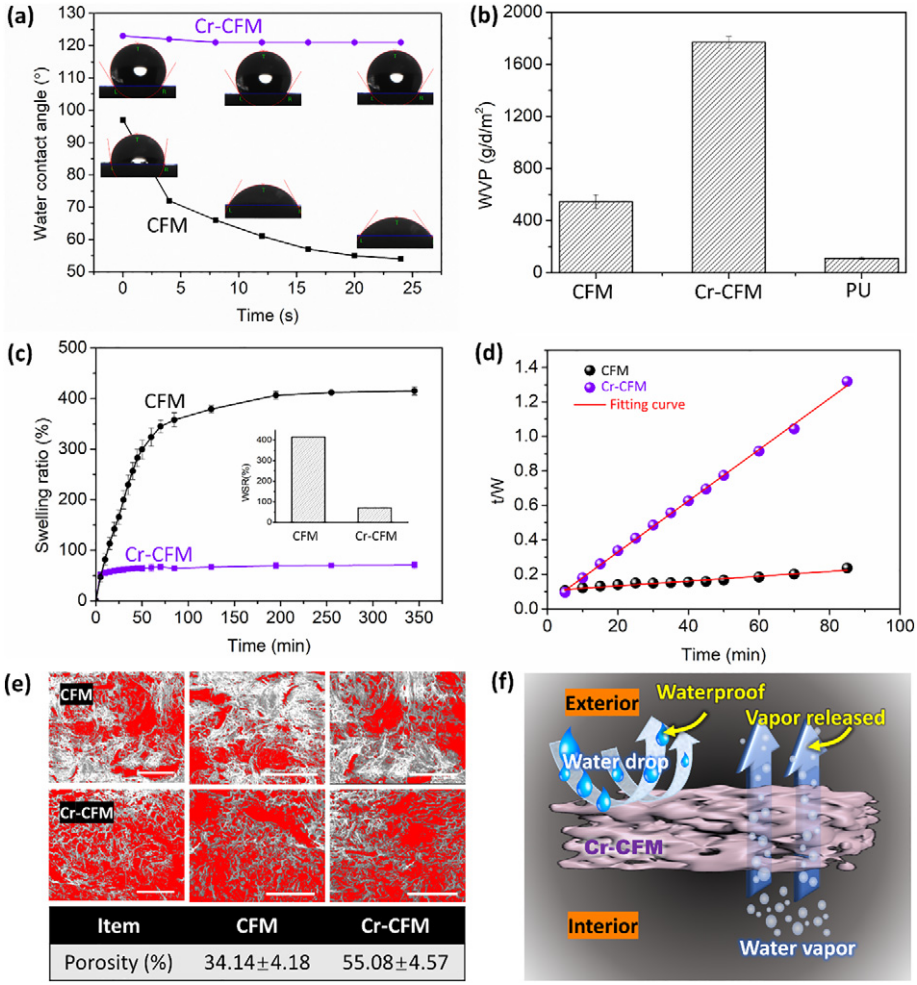

Fig. 3. (a) Water contact angle on surface of CFM and Cr-CFM with time; (b) water vapor permeability of CFM, Cr-CFM and commercial PU film; (c) water swelling ratio and (d) experimental data and fitting curves of second-order kinetics for CFM and Cr-CFM; (e) porosity results of CFM and Cr-CFM; (f) scheme of waterproofness and breathability of Cr-CFM.

the broken fibrous structure of Cr-CFM at different scale. The Mod 1 corresponds to the alignment of fibril along the pulling direction. This process involves broken of hydrogen bonds, electrovalent bonding, and shear force between fibrils, which leads to the toe region of strain–stress curve. After that, the fibril would enter an elastic region where the collagen molecules display a higher strain level in the gap than in the overlap region because of the lower molecular density. Around 13% of deformation, the sliding between the molecules becomes favorable. Followed is the molecular distortion and final cleavage of cross linkages [45] and collagen molecules backbones (Mod 3). Compared with CFM, Cr-CFM exhibits a smaller young's modulus and a steadier Mod 3. The reduced young's modulus may due to that Cr-CFM has a looser fibrous network and higher porosity. The enhancement in porosity may be caused by chromium complexing which lead to rearranges of collagen fiber, making the structure slack and uniform. It is also noticed that Cr-CFM has a higher elongation than CFM. This may because that the chromium linkages can work as core of fibril to sustain most of load.

The effect of hydration process on mechanical properties of Cr-CFM was investigated (Fig. 4c). It is notable that Cr-CFM exhibit water-adaptive mechanical property. After hydration, the strain-stress curve of Cr-CFM behaves more elastically, which is rather obvious by wetting for 90 min. The variations of characteristic features of mechanical property (young's modulus, stress and elongation at break) against wetting time are shown in Fig. 4d. With increasing wetting time, young's modulus and stress at break of Cr-CFM gradually decreased. This may because water molecules can break the hydrogen bonds, thereby reducing the interactions and shear forces between collagen fibers. Nevertheless, free water can work as lubricant while bonded water may act as bridge bonds between collagen when chains slide during stretching [35], resulting in slight increase of elongation at break. Hence, it can be concluded that Cr-CFM possesses tunable mechanical behaviors with water adaptability.

3.4. Shape memory ability

To demonstrate the shape memory behavior, straight Cr-CFM was immersed in water, then wrapped into a spiral shape on a glass rod (Fig. 5a) for shape deformation. After drying, the deformed Cr-CFM was taken off from the glass rod. It can be seen that the spiral shape of Cr-CFM was almost completely fixed, indicating its high shape fixing ability. Subsequently, the spiral trip was immersed in water and gradually returned to its original straight shape. The quantitative studied of shape memory ability of CFM and Cr-CFM was conducted through a stretch-recovery programming (Fig. 5b). In comparison to CFM (Fig. S2) of which the residual strain (22.5%) after first stretch is too high to perform subsequent cycle test, Cr-CFM (Fig. 5c) exhibits the curves with high degree of consistency after the first cycle, which consistent to typical stress-strain curves of stimuli-driven shape memory polymers [20]. Since Cr-CFM has a heterogeneous fibrous structure, the stress difference between first and subsequent loading process may result from orientation of random chains and strain-induced rearrangement of cross linkages that can work as netpoints in matrix and

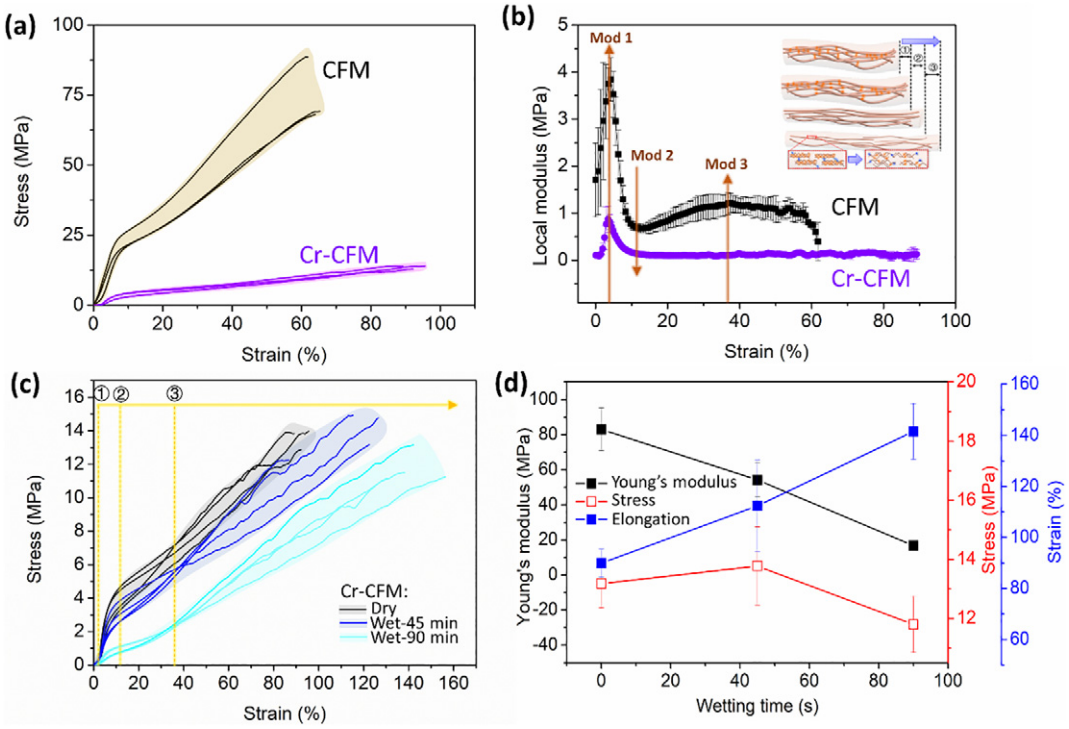

Fig. 4. (a) Strain-stress curves of CFM and Cr-CFM; (b) elastic modulus as a function of strain applied on CFM and Cr-CFM; (c) strain-stress curves of Cr-CFM under different wetting time; (d) young's modulus, stress and elongation at break of Cr-CFM with increasing wetting time.

lead to a more uniform network. During the three cycles, shape fixation ratio (R_f) of Cr-CFM increased from 69.2% to75.0%, while shape recovery ratio (R_r) increased from 64.7% to 99.3% (Table S1). Such shape memory ability in stretching dimension of Cr-CFM is not realized for CFM as its R_r has already fallen to 24.4% at second stretching cycle (Table S1). Corresponding variations of strain and stress of Cr-CFM under the five steps of shape memory programming are plotted in Fig. 5d. After immersing in water (step ①), Cr-CFM was stretched from a strain of 0% to 25% (step ②), meanwhile the stress increased from 0 MPa to 1.7 MPa. During later drying process (step ③), the stress gradually decreased to ~0 MPa with unchanged strain, implying fixation of setting elongation. Upon wetting again (step ④), the deformed Cr-CFM can recovery to a certain length without external force (Step ⑤) before next testing cycle. This process was repeated three times and showed a relatively stable circulation, which suggests the reusability of Cr-CFM as shape memory materials. The hysteresis test of Cr-CFM under moisture state further proves that Cr-CFM exhibit good stretchability and recovery in moisture environment in-situ (Fig. S3). Another programming (Fig. 5e) was also applied on Cr-CFM to demonstrate its editability regarding to shape memory ability. Results of R_f and R_r are summered in Fig. 5f. In the case of bending deformation, Cr-CFM also showed high R_f and R_r during the testing cycles. Particularly, R_f reached nearly 100% at third cycles while R_r maintained at 80%. Overall, Cr-CFM possesses water-responsive shape memory ability which has never been reported in other studies.

3.5. Shape memory mechanism

Herein, the mechanism of shape memory behavior of Cr-CFM was tried to be revealed by several characterization methods. FTIR was used to investigate effect of water molecules as stimulations on Cr-CFM from the viewpoint of shape memory programming. As shown in Fig. 6a, a broad absorption band at around 3290 cm^{-1} are evidently different for Cr-CFM in dry (original, deformation, and recovery) and wet (deformation, recovery). The peak become broader at wet condition due to existence of polar group of –OH from free water molecule. Regarding to wavenumber shifting, the peak shifted from 3288 cm^{-1} to 3300 cm^{-1} from wet to dry states and vice versa [40]. Similarly, compared to Cr-CFM in dry (original, deformation, and recovery), characteristic peaks of C═O stretching (Amide band I) and N—H bending (Amide band II) vibrations of Cr-CFM in wet (deformation, recovery) are found to be shifted to higher wavenumbers (Fig. 6b). During the wet and dry transitions, the peaks reversibly shift back and forth, indicating the cleavage and re-formation of hydrogen bonds within Cr-CFM under interference of water molecules [46]. Such behavior indicates the typical bonds with "switch" function. Specifically, cleavage of hydrogen bonds represents the "switch-on" state to allow deformation, while re-formation of hydrogen bonds denotes the "switch-off" state to lock temporary shape.

Change in elastic modulus (E′) subjected to a heating process for Cr-CFM under dry and wet condition was demonstrated from 22 °C to 120 °C using DMA. As shown in Fig. 6c, at room temperature, Cr-CFM in wet state has much lower E′ than dry state since the presence of water molecules destroys hydrogen bonds within collagen, causing the relaxation of matrix and increased flexibility of molecules. As temperature increases, E′ of dry Cr-CFM shows a slightly rise while E′ of wet Cr-CFM remains stable until the temperature reached 80 °C at which E′ starts to increase significantly and reach approximately the same value of dry Cr-CFM at 120 °C. it is suggested that as water molecules are gradually removed by heating, collagen interior hydrogen bonds can be re-formed again, leading to recovery of stiffness of matrix. Thus, the results confirm that water can stimuli the variation of hydrogen bonds within collagen, resulting in changes of mechanical modulus, which contributes to shape deformation and fixation for shape memory behavior.

The effect of length of the stimulating time on structure of Cr-CFM are evaluated by TGA. From the DTGA results (Fig. 6d) derived from TGA curves (Fig. S4), it can be seen that the first peak become broader and shifted to higher temperature region with increasing wetting time. Additionally, the main decomposition peak of collagen matrix shifted to higher temperature region with slower decomposition rate.

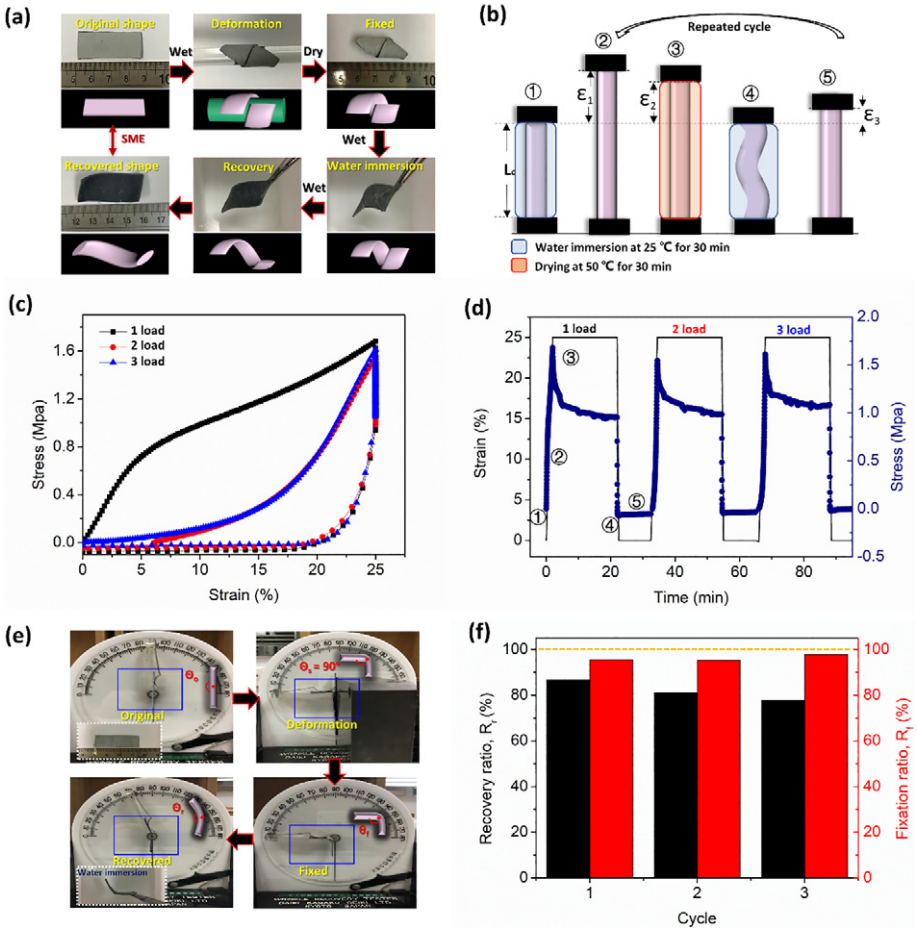

Fig. 5. (a) Water-responsive shape memory behavior of Cr-CFM; (b) stretching shape memory programming; (c) experimental results of cyclic tensile of Cr-CFM; (d) two-dimensional demonstration against wetting and drying cycle by the function of strain, stress with time; (e) stretching shape memory programming; (f) shape fixation ratio R_f and shape recovery ratio R_f under bending cycle.

These trends may come from several factors. On the one hand, longer wetting time leads to higher content of water. Meanwhile, chromium itself might provide some hydrogen bonding sites for water [47] and thus to prevent escaping of water from the matrix. On the other hand, under heating of high temperature, there may exist thermal-crosslinking effect between existing chromium and its adjacent collagen [48], which promotes the formation of more stable cross-linking network of Cr-CFM. In summary, the recovery of value of E′ from wet to dry state and increased thermal stability of Cr-CFM indicate that water cannot destruct the structure Cr-CFM on molecular level. In other words, it is reasonable to regard chromium-collagen complexing bonds as stable "netpoint" since it will not be impacted by stimuli of hydration.

Accordingly, the proposed mechanism of shape memory behavior of Cr-CFM is shown in Fig. 6e. Chromium complexing bond is regarded as "netpoint" due to their stability and strong bonding strength while hydrogen bonds within collagen molecule chains work as "switch". Upon external stimulation of water molecules (hydration process), inter-collagen hydrogen bonds can be cleaved, namely "switch-on" state, allowing shape deformation (U shape) of Cr-CFM from original shape (straight shape). The subsequent drying process leads Cr-CFM into "switch-off" state when the U shape is totally fixed. Once encountering water again, original shape of Cr-CFM can be restored with the help of osmotic pressure, swelling force and entropic stress from chromium-collagen linkages. Herein, the potential application of Cr-CFM is suggested. As illustrated in Fig. S5, a shape memory device of waist support belt can be developed. This belt is supposed to adapt to body under different condition. In addition, the in vitro cytotoxicity of Cr-CFM was evaluated (Fig. S6). It shows that Cr-CFM has moderate cytotoxicity, which implies its rationality in biomedical application.

4. Conclusions

Chromium (III) was successfully complexed with collagen fibrous matrix (CFM) without destroying collagen conformation and its original fiber morphology in the skin. The crosslinked structure on surface resulted in improved waterproofness of Cr-CFM, while the existence of three-dimensional (3D) microvoid in Cr-CFM endows its superior breathability. Compared to pristine CFM, Cr-CFM exhibited integrated strength and ductility due to existence of Chromium (III). Moreover, co-existence of hydrogen bonds and chromium (III) complexing linkages led to water-adaptive mechanical behaviors of Cr-CFM. Notably, such organic-metal biosystem of Cr-CFM achieved a completely athermal water-responsive shape memory ability with high shape fixation and recovery (>80%) during repeatable memory cycles. It is found that the temporary shape of Cr-CFM can be locked and released by reversible cleavage-reformation of hydrogen bonds under water interference, meanwhile shape recovery process happens as a result of entropic stress from stable chromium-collagen linkages, together with help of osmotic pressure and swelling force. Such design of organic-metal biosystem may provide an option for novel shape memory devices, biomimetic actuators and smart coatings, as well as bring new sights into smart functionality of protein materials.

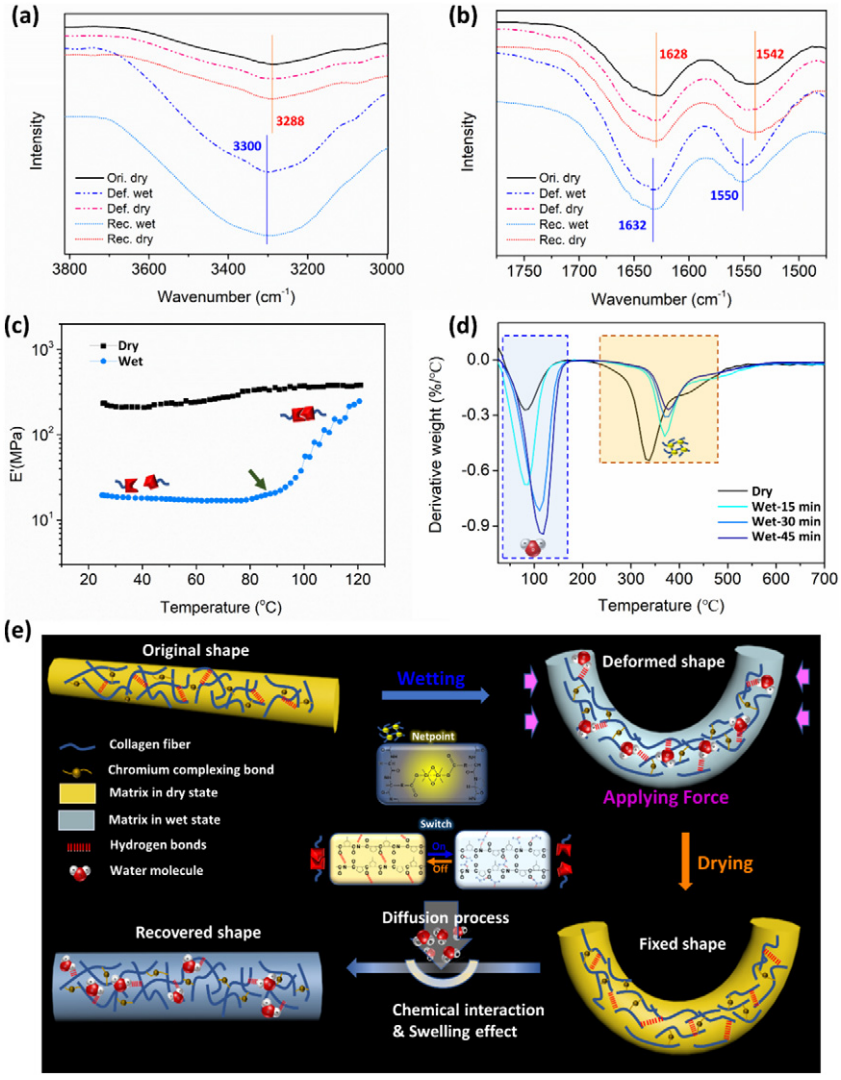

Fig. 6. FTIR characterization in the region of (a) 3000–3800 cm^{-1} and (b) 1500–1750 cm^{-1} of Cr-CFM in shape memory programming steps under dry and wet state (Ori.dry: original in dry state; Def.wet: deformation in wet state; Fix. dry: fixation in dry state; Rec.wet: recovery in wet state; Rec. dry: recovery in dry state); (c) E′ for Cr-CFM under dry and wet state as a function of temperature; (d) DTGA curves of Cr-CFM with different wetting time; (e) proposed switchable water-responsive shape-memory mechanism of Cr-CFM.

CRediT authorship contribution statement

Yanting Han: Conceptualization, Investigation, Formal analysis, Writing - original draft. **Yuanzhang Jiang:** Investigation, Formal analysis. **Jinlian Hu:** Conceptualization, Supervision, Writing - original draft. **Xiaoyu Chen:** Investigation.

Declaration of competing interest

There are no conflicts to declare.

Acknowledgements

This work is supported by the National Natural Science Foundation of China (51373147 and 51673162), Hong Kong General Research Fund (RGC No. 15209815) and Hong Kong PhD Fellowship (PF15-15110).

Appendix A. Supplementary data

Supplementary data to this article can be found online at https://doi.org/10.1016/j.matdes.2019.108206.

References

[1] M.J. Buehler, S. Keten, T. Ackbarow, Theoretical and computational hierarchical nanomechanics of protein materials: deformation and fracture, Prog. Mater. Sci. 53 (8) (2008) 1101–1241.
[2] C.-I. Brändén, J. Tooze, Introduction to Protein Structure, Taylor & Francis, 1999.
[3] D. Eisenberg, The discovery of the α-helix and β-sheet, the principal structural features of proteins, Proc. Natl. Acad. Sci. 100 (20) (2003) 11207–11210.
[4] S.-W. Chang, M.J. Buehler, Molecular biomechanics of collagen molecules, Mater. Today 17 (2) (2014) 70–76.
[5] S.P. Veres, J.M. Harrison, J.M. Lee, Mechanically overloading collagen fibrils uncoils collagen molecules, placing them in a stable, denatured state, Matrix Biol. 33 (2014) 54–59.
[6] S. Riedel, P. Hietschold, C. Krömmelbein, T. Kunschmann, R. Konieczny, W. Knolle, C.T. Mierke, M. Zink, S.G. Mayr, Design of biomimetic collagen matrices by reagent-free electron beam induced crosslinking: structure-property relationships and cellular response, Mater. Des. 168 (2019), 107606.
[7] D. Gopinath, M.R. Ahmed, K. Gomathi, K. Chitra, P. Sehgal, R. Jayakumar, Dermal wound healing processes with curcumin incorporated collagen films, Biomaterials 25 (10) (2004) 1911–1917.
[8] W. Han, S. Chen, W. Yuan, Q. Fan, J. Tian, X. Wang, L. Chen, X. Zhang, W. Wei, R. Liu, Oriented collagen fibers direct tumor cell intravasation, Proc. Natl. Acad. Sci. 113 (40) (2016) 11208–11213.
[9] Z. Liu, M.A. Meyers, Z. Zhang, R.O. Ritchie, Functional gradients and heterogeneities in biological materials: design principles, functions, and bioinspired applications, Prog. Mater. Sci. 88 (2017) 467–498.
[10] P.F. Gratzer, K. Conlan, A. Murphy, A new decellularized dermal matrix: superior properties and in-vivo performance when compared with the leading commercial product, Front. Bioeng. Biotechnol. 01 (01) (2016).

[11] C. Zhang, D.A. Mcadams, J.C. Grunlan, Nano/micro-manufacturing of bioinspired materials: a review of methods to mimic natural structures, Adv. Mater. 28 (30) (2016) 6292–6321.
[12] A. Yarin, Coaxial electrospinning and emulsion electrospinning of core–shell fibers, Polym. Adv. Technol. 22 (3) (2011) 310–317.
[13] C.-L. Zhang, S.-H. Yu, Nanoparticles meet electrospinning: recent advances and future prospects, Chem. Soc. Rev. 43 (13) (2014) 4423–4448.
[14] M.T. Wolf, K.A. Daly, E.P. Brennan-Pierce, S.A. Johnson, C.A. Carruthers, A. D'Amore, S.P. Nagarkar, S.S. Velankar, S.F. Badylak, A hydrogel derived from decellularized dermal extracellular matrix, Biomaterials 33 (29) (2012) 7028–7038.
[15] Z. Su, H. Ma, Z. Wu, H. Zeng, Z. Li, Y. Wang, G. Liu, B. Xu, Y. Lin, P. Zhang, Enhancement of skin wound healing with decellularized scaffolds loaded with hyaluronic acid and epidermal growth factor, Mater. Sci. Eng. C 44 (2014) 440–448.
[16] P. Cole, T.W. Horn, S. Thaller, The use of decellularized dermal grafting (AlloDerm) in persistent oro-nasal fistulas after tertiary cleft palate repair, J. Craniofac. Surg. 17 (4) (2006) 636–641.
[17] X. Qiu, S. Hu, "Smart" materials based on cellulose: a review of the preparations, properties, and applications, Materials 6 (3) (2013) 738–781.
[18] L.E. O'leary, J.A. Fallas, E.L. Bakota, M.K. Kang, J.D. Hartgerink, Multi-hierarchical self-assembly of a collagen mimetic peptide from triple helix to nanofibre and hydrogel, Nat. Chem. 3 (10) (2011) 821.
[19] Y. Han, J. Hu, L. Jiang, Collagen skin, a water-sensitive shape memory material, J. Mater. Chem. B 6 (31) (2018) 5144–5152.
[20] J. Hu, Y. Zhu, H. Huang, J. Lu, Recent advances in shape–memory polymers: structure, mechanism, functionality, modeling and applications, Prog. Polym. Sci. 37 (12) (2012) 1720–1763.
[21] Y. Lu, N. Yeung, N. Sieracki, N.M. Marshall, Design of functional metalloproteins, Nature 460 (7257) (2009) 855.
[22] A. Michalak, M. Mitoraj, T. Ziegler, Bond orbitals from chemical valence theory, J. Phys. Chem. A 112 (9) (2008) 1933–1939.
[23] E.H. Nashy, O. Osman, A.A. Mahmoud, M. Ibrahim, Molecular spectroscopic study for suggested mechanism of chrome tanned leather, Spectrochim. Acta A Mol. Biomol. Spectrosc. 88 (2012) 171–176.
[24] Y. Zhang, T. Snow, A.J. Smith, G. Holmes, S. Prabakar, A guide to high-efficiency chromium (III)-collagen cross-linking: synchrotron SAXS and DSC study, Int. J. Biol. Macromol. 126 (2019) 123–129.
[25] A. Macfie, E. Hagan, A. Zhitkovich, Mechanism of DNA— protein cross-linking by chromium, Chem. Res. Toxicol. 23 (2) (2009) 341–347.
[26] K. Salnikow, A. Zhitkovich, M. Costa, Analysis of the binding sites of chromium to DNA and protein in vitro and in intact cells, Carcinogenesis 13 (12) (1992) 2341–2346.
[27] Y. Zhu, J. Hu, H. Luo, R.J. Young, L. Deng, S. Zhang, Y. Fan, G. Ye, Rapidly switchable water-sensitive shape-memory cellulose/elastomer nano-composites, Soft Matter 8 (8) (2012) 2509–2517.
[28] L. He, C. Mu, J. Shi, Q. Zhang, B. Shi, W. Lin, Modification of collagen with a natural cross-linker, procyanidin, Int. J. Biol. Macromol. 48 (2) (2011) 354–359.
[29] G. Tronci, A. Doyle, S.J. Russell, D.J. Wood, Triple-helical collagen hydrogels via covalent aromatic functionalisation with 1, 3-phenylenediacetic acid, J. Mater. Chem. B 1 (40) (2013) 5478–5488.
[30] Q. Yao, Y. Wang, H. Chen, H. Huang, B. Liu, Mechanism of high chrome uptake of tanning pickled pelt by carboxyl-terminated hyper-branched polymer combination chrome tanning, ChemistrySelect 4 (2) (2019) 670–680.
[31] L. Li, D.Y. Kim, G.M. Swain, Transient formation of chromate in trivalent chromium process (TCP) coatings on AA2024 as probed by Raman spectroscopy, J. Electrochem. Soc. 159 (8) (2012) C326–C333.
[32] H. Vašková, Raman microscopic detection of chromium compounds, MATEC Web of Conferences 20th International Conference on Circuits, Systems, Communications and Computers (CSCC 2016), EDP Sciences, 2016.
[33] C.A. Maxwell, T.J. Wess, C.J. Kennedy, X-ray diffraction study into the effects of liming on the structure of collagen, Biomacromolecules 7 (8) (2006) 2321–2326.
[34] S. Jeyapalina, G.E. Attenburrow, A.D. Covington, Dynamic mechanical thermal analysis (DMTA) of leather part 1: effect of tanning agent on the glass transition temperature of collagen, J. Soc. Leather Technol. Chem. 91 (6) (2007) 236–242.
[35] M. Schroepfer, M. Meyer, DSC investigation of bovine hide collagen at varying degrees of crosslinking and humidities, Int. J. Biol. Macromol. 103 (2017) 120–128.
[36] J.P. Orgel, T.C. Irving, A. Miller, T.J. Wess, Microfibrillar structure of type I collagen in situ, Proc. Natl. Acad. Sci. 103 (24) (2006) 9001–9005.
[37] M. Liu, J. Ma, B. Lyu, D. Gao, J. Zhang, Enhancement of chromium uptake in tanning process of goat garment leather using nanocomposite, J. Clean. Prod. 133 (2016) 487–494.
[38] J. Hu, Y. Wu, C. Zhang, B.Z. Tang, S. Chen, Self-adaptive water vapor permeability and its hydrogen bonding switches of bio-inspired polymer thin films, Mater. Chem. Front. 1 (10) (2017) 2027–2030.
[39] H. Schott, Swelling kinetics of polymers, J. Macromol. Sci., Part B: Phys. 31 (1) (1992) 1–9.
[40] Y. Han, J. Hu, X. Chen, A skin inspired bio-smart composite with water responsive shape memory ability, Mater. Chem. Front 3 (2019) 1128–1138.
[41] M.J. Buehler, Y.C. Yung, Deformation and failure of protein materials in physiologically extreme conditions and disease, Nat. Mater. 8 (3) (2009) 175.
[42] W. Yang, V.R. Sherman, B. Gludovatz, E. Schaible, P. Stewart, R.O. Ritchie, M.A. Meyers, On the tear resistance of skin, Nat. Commun. 6 (2015) 6649.
[43] B. Depalle, Z. Qin, S.J. Shefelbine, M.J. Buehler, Influence of cross-link structure, density and mechanical properties in the mesoscale deformation mechanisms of collagen fibrils, J. Mech. Behav. Biomed. Mater. 52 (2015) 1–13.
[44] M.J. Buehler, T. Ackbarow, Fracture mechanics of protein materials, Mater. Today 10 (9) (2007) 46–58.
[45] A.L. Kwansa, R. De Vita, J.W. Freeman, Mechanical recruitment of N-and C-crosslinks in collagen type I, Matrix Biol. 34 (2014) 161–169.
[46] A. Haroun, R. Masoud, S. Bronco, Synthesis of Citric Acrylate Oligomer and Its In-situ Reaction With Chrome Tanned Collagen (Hide Powder), Macromolecular Symposia, Wiley Online Library, 2006 187–194.
[47] J.-H. Choi, I.-G. Oh, K.S. Ryoo, W.-T. Lim, Y.C. Park, M.H. Habibi, Structural and spectroscopic properties of trans-difluoro (1, 4, 8, 12-tetraazacyclopentadecane) chromium (III) perchlorate hydrate, Spectrochim. Acta A Mol. Biomol. Spectrosc. 65 (5) (2006) 1138–1143.
[48] R. Usha, T. Ramasami, Effect of crosslinking agents (basic chromium sulfate and formaldehyde) on the thermal and thermomechanical stability of rat tail tendon collagen fibre, Thermochim. Acta 356 (1–2) (2000) 59–66.